

# Plasma-Activated Sintering of Aluminum Nitride

J.E. Hensley, Jr., S.H. Risbud, J.R. Groza, and K. Yamazaki

The use of a new plasma-activated sintering (PAS) process to densify aluminum nitride (AlN) powders to nearly full theoretical density (97 to >99%) in 5 to 10 min was investigated. The process consists of a pulse activation step, followed by sintering at 1730 to 1800 °C using resistance heating in carbon dies. Submicron size (~0.44 μm) AlN powders of low oxygen content (<1 wt%) were consolidated to near full density in both air and vacuum with no sintering aids or binders. Transmission electron microscopy (TEM) examination revealed an equiaxed, submicron grain structure (~0.77 μm) with no apparent pores or intergranular phases. X-ray powder diffraction revealed no secondary crystalline phases.

## Keywords

AlN, densification, density, grain structure, intergranular phases, plasma, powder consolidation, sintering, thermal conductivity

## 1. Introduction

THE use of aluminum nitride (AlN) in electronic packaging provides a significant improvement compared to the traditional packaging material alumina (Al<sub>2</sub>O<sub>3</sub>).<sup>[1,2]</sup> The thermal conductivity of AlN (>150 W/m · K) is higher than iron (78 W/m · K) and much higher than alumina (30 W/m · K). This improves the reliability of the electronic systems by reducing the self-heating of densely arrayed electronic devices. AlN has good electrical insulation properties, with electrical conductivity of 10<sup>-11</sup> to 10<sup>-13</sup> Ω<sup>-1</sup> m<sup>-1</sup> and a relative dielectric constant of 8 to 8.5. It also has high strength, and the thermal expansion of AlN (3.9 mK<sup>-1</sup>) closely matches silicon (3.0 mK<sup>-1</sup>).

Aluminum nitride is a covalently bonded compound that crystallizes in the hexagonal wurtzite structure.<sup>[1]</sup> At low temperatures, it has low atomic diffusion of aluminum and nitrogen. In air, oxidation starts at 997 °C, whereas under pure nitrogen at 100 kPa pressure, the material is stable up to 2517 ± 50 °C and decomposes at higher temperatures. This makes it a difficult material to sinter to its full density of 3.255 g/cm<sup>3</sup>. Presently, three broad categories of sintering methods have been used to sinter aluminum nitride successfully: pressureless sintering, hot pressing, and plasma sintering. In 1989, Kuramoto and co-workers<sup>[3]</sup> sintered aluminum nitride powder in a nitrogen atmosphere at 1850 °C in 7 h using pressureless sintering. They achieved a density of 98.7% and a mean grain size of 5 to 8 μm. In 1992, Teusel and Rüssel<sup>[4]</sup> reduced the sintering time to 3 h using additives of 10 wt% SiC and 2 wt% Y<sub>2</sub>O<sub>3</sub> at 1950 °C. They achieved a density of 97% and reduced the mean grain size to 3 μm. In 1991, Surnev and co-workers<sup>[5]</sup> used hot pressing with Y<sub>2</sub>O<sub>3</sub>, CaO, CaF<sub>2</sub>, and CaC<sub>2</sub> as additives to sinter AlN at 1500 °C. They achieved their highest thermal conductivity values with 1 wt% Y<sub>2</sub>O<sub>3</sub> and achieved 98% density. From a fractograph of the 0.5 wt% Y<sub>2</sub>O<sub>3</sub> + 0.5 wt% CaO, the authors estimate that they achieved an average grain size of about 0.8

μm. To reduce the sintering time, Knittel and Risbud<sup>[6]</sup> successfully used a microwave plasma to sinter AlN to 95% density in 15 min at 1500 °C. A 2% yttria addition was added to the powder and mixed with a binder. The powder was pressed in a green state and then sintered in the 100-torr nitrogen gas microwave plasma. The resulting mean grain size was 2 μm.

The improvements in densification rates of AlN have been the result of the addition of sintering aids, most notably, yttria. However, the desired properties of aluminum nitride as an electronic packaging material are only achieved if the resulting material is not only fully dense, but also as pure as possible. The presence of voids, impurities, and intergranular phases scatter phonons, which reduce the thermal conductivity. These lattice disruptions also lower the strength. The addition of more than 1 wt% oxygen rapidly reduces the thermal conductivity of AlN.<sup>[2]</sup> The presence of sintering aids, although improving the densification rates and lowering the sintering temperatures, has also reduced the overall thermal conductivity, *k*, as predicted by the dispersed phase model:<sup>[7]</sup>

$$\frac{k}{k_g} = \frac{3 - 2 \left( 1 + \frac{k_{gb}}{k_g} \right) f_{gb}}{3 + \left( \frac{k_g}{k_{gb}} - 1 \right) f_{gb}}$$

where *k<sub>g</sub>* is the thermal conductivity of the dispersed AlN grains; *k<sub>gb</sub>* is the average thermal conductivity of the grain boundary phase; and *f<sub>gb</sub>* is the volume fraction of the grain boundary phase.

The thermal conductivity of yttria (Y<sub>2</sub>O<sub>3</sub>) is 54 W/m · K. Because the yttria settles into the grain boundary during the sintering process, it increases the volume fraction of the grain boundary phase, *f<sub>gb</sub>*, and reduces the average thermal conductivity of the grain boundary phase, *k<sub>gb</sub>*. Thus, increasing amounts of additives have deleterious effects on the overall thermal conductivity. Consider an AlN sample with polycrystalline grains having a thermal conductivity of 260 and grain boundaries of Y<sub>2</sub>O<sub>3</sub> with thermal conductivity of 54. Assuming *k<sub>g</sub>* is 260, *k<sub>gb</sub>* is 54 and *f<sub>gb</sub>* is 0.05, the average thermal conductivity, *k*, of the material would be 238. This illustration assumes the thermal conductivity of the grain boundary phase to be that of pure yttria. In reality, it should be lower due to a polycrystalline phase with numerous defects and the presence of an amorphous phase. In their investigation, Surnev and others reported

J. Hensley, Jr., S.H. Risbud, and J.R. Groza, Division of Materials Science and Engineering, Department of Chemical Engineering and Materials Science; K. Yamazaki, Department of Mechanical, Aeronautical and Materials Engineering, University of California, Davis, Davis, CA 95616-5294.

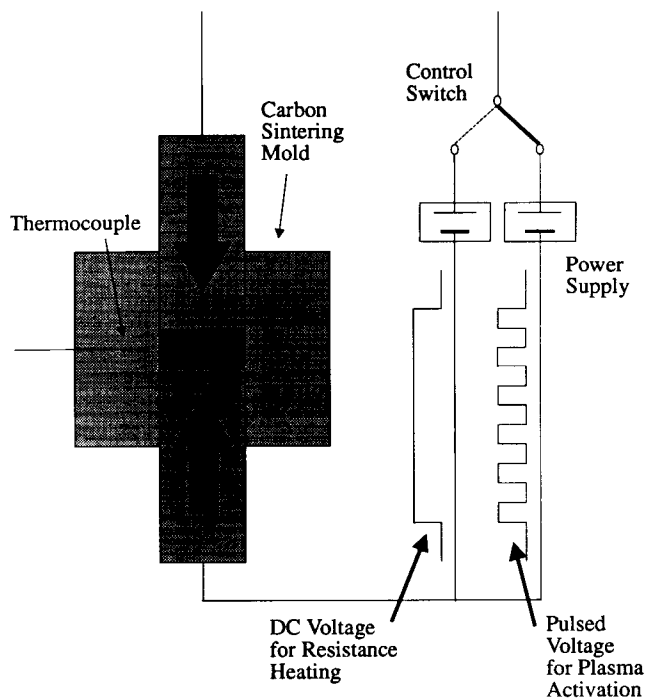


Fig. 1 Schematic of plasma-activated sintering process.

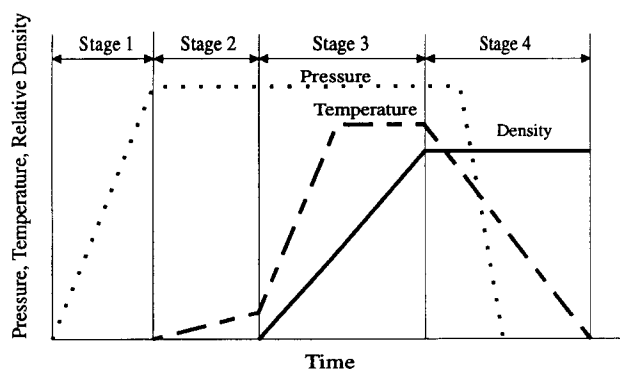


Fig. 2 Plasma-activated sintering pressure, temperature, and relative density profiles.

that the highest average thermal conductivity measured was 117 for AlN with the addition of 1 wt%  $Y_2O_3$ .<sup>[3]</sup> This value is significantly higher than the thermal conductivity of alumina at 30, but elimination of additives represents a clear means of obtaining even higher thermal conductivity values than 117.

The plasma-activated sintering process (PAS), developed by Sodick, Ltd., of Japan, was selected to reduce the need for additives and to rapidly and successfully sinter pure AlN. This process has been successfully used by Matsushita in a commercial capacity to sinter Fe-Nd-Co-B magnets<sup>[8]</sup> and by The University of California, Davis, to sinter additive-free AlN.<sup>[9]</sup> A schematic of the PAS process is shown in Fig. 1. The commercial powders are poured into the graphite carbon molds without additives, binders, or pre-pressing. Modest uniaxial pressure is applied to the powder, and an external power source provides a

Table 1 Typical PAS processing parameters

Applied pressure.....	15 MPa
Pulse voltage.....	25 V
Pulse current.....	750 A
Pulse on-state duration.....	80 ms
Pulse off-state duration.....	80 ms
Total pulse duration.....	30 s
Resistance heating voltage.....	70 V
Resistance heating current.....	2000 A
Total consolidation time.....	<10 min

pulsed plasma to activate the surface of the particles. The power supply is then switched to resistance heating for densification. To measure the sintering temperature, a thermocouple is inserted into the carbon mold, and a linear gage measures the shrinkage. A typical profile of temperature and pressure use in PAS is shown in Fig. 2. During stage 1, the pressure is applied to the powder. At stage 2, the pulse discharge is initiated, and some minor heating occurs as the particle surfaces are activated. At stage 3, the pulse plasma is removed, and resistance heating is started. Heating occurs, after the desired sintering temperature is reached, until shrinkage is complete. The pressure is then removed in stage 4. Typical parameters for PAS processing are shown in Table 1.

Three effects in the PAS process contribute to powder densification: electrical discharge, resistance heating, and mechanical pressure. Although the effects of pressure and temperature have received substantial attention and are well documented in existing models,<sup>[10,11]</sup> the understanding of the plasma contribution to densification is very limited. In particular, there is no study available on the plasma activation effect in PAS and the mechanism that provides such rapid densification.

Although a comprehensive explanation of the role of the plasma step in PAS is not yet available, the authors suggest the following preliminary theoretical framework. The plasma state is created during the application of the pulsed electrical current to the loose powder stack in the graphite die. Local high-density electrical discharges are produced at the contact points between the particles. These rapid microdischarges produce transient plasma phenomena that include ionization, thermal radiation, gas excitation, UV emission, and shock waves. In PAS, the typical current pulse has a density of about 100 A/cm<sup>2</sup>, with the global field along the powder column on the order of 100 V/cm. Based on this current density value, a plasma density of 10<sup>13</sup> cm<sup>-3</sup> may be estimated. At atmospheric pressure in air, the ionization process by plasma generation more likely involves valence electrons rather than lower level electrons. This single ionization level is estimated to be low, about 1 ion for 10<sup>6</sup> atoms, with neutral gas density much larger than gas plasma density. Also, the mean-free paths of molecular collisions with electrons, ions, other molecules, and the material body are smaller than the body dimensions (particles). In these conditions, a continuum (fluid) model for the plasma may be assumed that constitutes the basis for modeling the plasma heating effect for AlN.<sup>[12]</sup>

In this modeling, the electrons are assumed to equilibrate to a temperature,  $T_e$ , that is higher than that of the gas and ions because of their considerably smaller inertia. The gas, ions, and material bodies are assumed to be at a common temperature,  $T_s$ ,

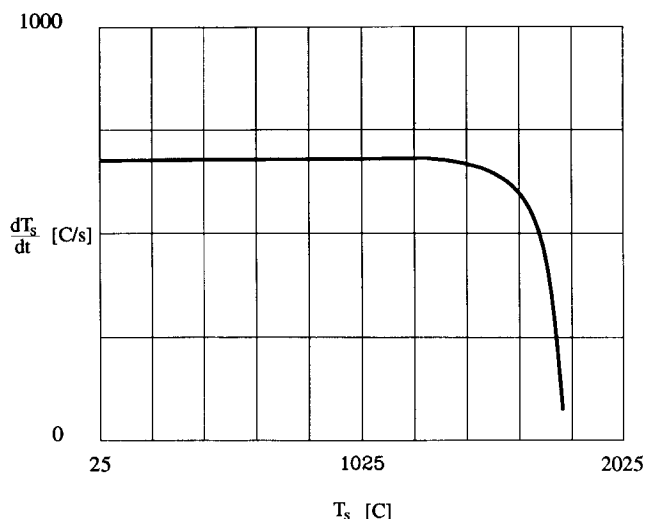


**Fig. 3** Temperature rate (°C/s) from heat balance model. Note that there is constant heat rate to 1600 °C.

An energy exchange is considered to take place between the random thermal fluxes carried by electrons and ions from the plasma toward the body and the thermal flux carried away from the body by the thermionic emission of electrons. In this preliminary model, a thermodynamic equilibrium with a steady flux condition for a continuum plasma and the thermionic emitter may be assumed to describe conditions within a small fraction of the total pulse time of an electrical discharge. The heating time to a target temperature and the heating rate for an initially cold particle are calculated from this net flux, based on continuous plasma-particle interaction. The result of this calculation for heating rate of AlN particles is shown in Fig. 3. Note that the heating rate is high and constant up to a temperature,  $T_s$ , of 1600 °C. In reality, steady state heating may only comprise a few percent of the time that the pulse discharge is applied. To heat particles significantly, a pulsed discharge must be applied for quite some time. Typically, in PAS, about 200 pulses are applied. In this case, one can estimate that the particle surface may reach temperatures of about 1600 °C in about 2.7 s if steady-state heating occurs for about 15% of each pulse duration. At these temperatures, full densification may occur without significant decomposition of AlN. The actual heating of the entire particle is intended to take place during the subsequent resistance heating; thus, pulse discharging is applied only to activate the powder particle surface.

This rapid and concentrated heating of the powder particle surface at temperatures of 1600 °C may be very effective in debonding the surface oxides and cleaning the sintering particle surface, thereby creating the activated AlN surface. Besides the heating effects, plasma localizes a higher energy density on the surface of the particles, which induces other physical and chemical processes that activate the particle surface, thus increasing the driving force for subsequent densification. For instance, the electron and ion bombardment on the particle surface may produce sputtering effects with outgassing and, again, cleaning of impurities, adsorbed gases, and moisture from the particle surface. The electronically excited gases may

**Table 2** Aluminum nitride powder elemental analysis

Element	Content, wt%
Al .....	65.4
N .....	33.5
Ca .....	34 ppm
Mg .....	...
Cr .....	...
Fe .....	<10 ppm
Si .....	<10 ppm
C .....	440 ppm
O .....	0.82

**Note:** Powder was provided by Tokuyama Soda Co., Ltd., for Lot No. 1257011 (grade F), June 21, 1991. Note the low content of impurities (Fe and Si) and less than 1 wt% oxygen. Other typical impurities (Mg and Cr) were apparently too low to detect.

also produce surface phenomena that activate powder particle surfaces. All of these effects take place for a short time during the pulse duration when microdischarges at particle contact points create local breakdown. The remaining time of the pulse involves voltage collapse when the high field diminishes and the plasma recombines most significantly on particle surfaces. Therefore, the efficiency of oxide breakdown and plasma cleaning effects increases by pulsing the electrical discharge rather than lengthening the plasma pulse duration. Considerable additional work is necessary to distinguish between the microdischarge time and heating time within a single pulse application during the electrical discharge stage and to quantify the other physical and chemical surface effects.

## 2. Experimental Procedure and Results

The AlN powder (Tokuyama Soda Co., Ltd., Japan) used for sintering was a grade F powder with a specific surface area of 3 to 4 m<sup>2</sup>/g, a mean crystallite size of 0.44 μm, and an agglomerated particle size of less than 2.0 μm. The particle size distribution was such that 70% of the particles were less than 3 μm in size. The chemical analysis of the powders is shown in Table 2. Magnesium, heavy metals chromium and iron, and silicon were less than 10 ppm. The modest carbon impurity, 440 ppm, resulted from the carbothermal reduction of alumina in the manufacturing process. Most importantly, the oxygen content was very low (less than 1 wt%).

Three samples were prepared by PAS. Each sample was 2 cm in diameter and about 2 mm thick. The first sample, sintered in air at 15.6 MPa at 1730 °C, reached full densification in 5 min. The second and third were sintered in vacuum of 5 mtorr at 14.0 MPa at 1600 and 1800 °C, respectively, and reached final densification in 4 min. These sintering times were significantly lower than those used in previous sintering methods and were accomplished without the use of sintering aids. The samples were examined using a TEM to evaluate grain size and microstructure. Hardness testing was performed on the 1730 °C sample. A powder X-ray diffractometer with Cu K<sub>α</sub> scanned 2θ angles of 20 to 50° to confirm the existence of AlN and identify any secondary phases. Density of the 1800 °C sample was measured using the Archimedes principle.



**Fig. 4** Microstructure of AlN sintered at 1730 °C with 15.6 MPa for 5 min in air with no sintering additives. Note the equiaxed polycrystalline structure with no apparent porosity. The mean grain size is  $0.77 \pm 0.1 \mu\text{m}$ .

The resulting microstructure of the 1730 °C sample is shown in Fig. 4. The equiaxed grains have an average grain size of  $0.77 \mu\text{m}$ . This 75% increase over the original powder size of  $0.44 \mu\text{m}$  is quite small compared with the considerably larger grain coarsening observed in conventional sintering studies of undoped AlN (about 1000% increase in Ref 1). Examination of the microstructure reveals no apparent porosity or intergranular phases, and diffraction patterns revealed a polycrystalline structure. The microhardness yielded  $8188 \pm 73 \text{ MPa}$ . The powder X-ray diffraction results of the 1600 °C sample are presented in Table 3. The measured and theoretical values of interplanar spacings and relative intensities show good correlation for the three strongest peaks. The existence of the weak fourth peak at very small spacing is not yet understood, although it is less likely to describe a secondary crystalline phase. Density of the 1730 °C sample was >99%, whereas that of the 1800 °C sample was 97%.

### 3. Conclusions and Further Work

The use of plasma-activated sintering (PAS) of aluminum nitride has yielded encouraging results. Near full density (97 to >99%) was achieved with a significant reduction in sintering time and without the use of sintering aid additives. Minimal

**Table 3** X-ray powder diffraction results for AlN sintered at 1600 °C with 14.0 MPa for 4 min in vacuum of 5 mtorr with no sintering additives

$d$ (theoretical)(a)	$I/I_0$ (theoretical)(a)	$d$ (measured)	$I/I_0$ (measured)
2.70 .....	100	2.6938	100.0
2.37 .....	70	2.3691	74.8
2.49 .....	60	2.4896	62.0
... ..	...	1.8279	25.8

**Note:** The data correspond very well to the three reported peaks of the AlN powder diffraction file. The existence of the fourth peak is, as yet, unexplained. (a) From NBS Powder Diffraction File 8-262 (AlN).

coarsening and grain growth occurred in the rapid (less than 10 min) PAS process. Significant work remains to be done to further reduce the time and temperature and achieve the maximum densification. This will best be achieved by a thorough understanding of the consolidation mechanism involved. The nature and role of the plasma in sintering is not yet understood. Sophisticated microstructural investigations by electron microscopy are needed for a better understanding of the consolidation mechanism in PAS. Further study of the grain boundaries is required by image analysis using a high-voltage electron microscope (HVEM) and microchemistry techniques. A better understanding of the consolidation mechanism will allow optimization of the processing parameters, such as plasma application time and voltage, pressure, resistance heating current, and sintering temperature, to achieve the highest quality aluminum nitride materials.

### Acknowledgments

This work is based on part of the M.S. thesis of J.E. Hensley, Jr. at UC-Davis. The authors also wish to thank Sundeep Rele of Ceracon, Inc. of Sacramento, California, for assistance in the density measurements.

### References

1. D. Bloor, R.J. Brook, M.C. Flemings, and S. Mahajan, Ed., *Encyclopedia of Advanced Materials*, Pergamon Press, 1993
2. R.R. Tummala and E.J. Rymaszewski, *Microelectronics Packaging Handbook*, Van Nostrand-Reinhold, 1989, p 492-510
3. N. Kuramoto, H. Taniguchi, and L. Aso, Development of Translucent Aluminum Nitride Ceramics, *Ceram. Bull.*, Vol 68 (No. 4), 1989, p 883-887
4. I. Teusel and C. Rüsel, Pressureless Sintering of Aluminum Nitride/Silicon Carbide Ceramics, *J. Mater. Sci. Lett.*, Vol 11 (No. 4), 1992, p 205-207
5. S. Surnev, D. Lepkova, and A. Yoleva, Influence of Sintering Additives on the Phase Composition and the Thermal Conductivity of Aluminum Nitride Ceramics, *Mater. Sci. Eng. B*, Vol 10 (No. 1), 1991, p 35-40
6. S.M. Knittel and S.H. Risbud, Microwave Plasma Densification of Aluminum Nitride, *Combustion and Plasma Synthesis of High Temperature Materials*, Z.A. Munir and J.B. Holt, Ed., VCH Publishers, 1990, p 414-419
7. D.R. Flynn, in *Mechanical and Thermal Properties of Ceramics*, B. Wachtman, Jr., Ed., NBS Spec. Publ. 303, 1969
8. M. Wada and F. Yamashita, "New Method of Making Nd-Fe-Co-B Fully Dense Magnet," *Intermag. Conf. Proc.*, 1990, GP-07

9. J. Groza, S.H. Risbud, and K. Yamazaki, Plasma Activated Sintering of Additive-Free AlN Powders to Near-Theoretical Density in 5 Minutes, *J. Mater. Res.*, Vol 7 (No. 10), 1992, p 2643-2645
10. M.F. Ashby, A First Report on Sintering Diagrams, *Acta Metall.*, Vol 22 (No. 3), 1974, p 275-289
11. A.S. Helle, K.E. Easterling, and M.F. Ashby, Hot-Isostatic Pressing Diagrams: New Developments, *Acta Metall.*, Vol 33 (No. 12), 1985, p 2163-2174
12. M. Garcia, "Plasma Sintering: Comments on the Plasma Effects," Lawrence Livermore National Laboratory Internal Report, Feb 7, 1993